

PREDICTING PRESSURE DROP IN PNEUMATIC CONVEYING USING THE DISCRETE ELEMENT MODELLING APPROACH

V SINGH and SIMON LO

CD-adapco, Trident House, Basil Hill Road, Didcot, OX11 7HJ, UK.

ABSTRACT

Pneumatic conveying of solid materials is used in many process industries where solid particles are carried forward in pipes and channels by the fluid. Accurate prediction of pressure drop across the conveying system is essential in determining the optimum operating parameters for a smooth conveying operation. The pressure drop in the system is dependent on a host of parameters such as particle and pipe diameters, particle and fluid properties, pipe roughness and orientation, etc. In this study, the commercial CFD software, STAR-CD is used to model pneumatic conveying in a horizontal pipe. The fluid phase is modelled using the Reynolds averaged Navier-Stokes equations and k-epsilon model for turbulent flow. The particles are modelled as discrete elements. The DEM (Discrete Element Modelling) module in STAR-CD is used to study the particle flow and to predict the pressure drop in the pipe. The flow system studied consists of a horizontal pipe with an internal diameter of 52.6 mm. Mono-sized spherical particles are injected uniformly at the pipe inlet. A range of fluid flow rates is studied. Reasonable agreement is obtained between the predicted pressure drop and the experimental data of Marcus et al. Sensitivity of the computed results to particle properties and the choice of fluid drag model is also studied.

NOMENCLATURE

- A Constant in expression for C_D
 B Constant in expression for C_D
 C Constant in expression for C_D
 D Constant in expression for C_D
 A_p Projected area of particle.
 C_D Drag Coefficient.
 \vec{F} Force vector acting on particle.
 \vec{g} Acceleration due to gravity.
 I_i Mass moment of Inertia of particle 'i'.
 m_i Mass of particle 'i'.
 R Rotation matrix.
 Re Reynolds number.
 \vec{v}_i Velocity vector of particle 'i'.
 \vec{v}_f Fluid velocity vector.
 $\vec{\tau}_i^B$ Net torque acting on particle 'i' in body ref. frame.

ρ_f Fluid density.

$\vec{\omega}_i$ Angular velocity vector of particle 'i'.

INTRODUCTION

Pressure drop in pneumatic conveying has received attention from numerous researchers, who have presented a host of experimental data [Tsuji and Morikawa, 1982] as well as correlations related to pressure drop. Several recent studies on diluted conveying [Lain and Sommerfeld 2008, Vasquez et al 2008] have adopted CFD to predict pressure drop in pipes and channels. It has been shown that increasing wall friction [Lain and Sommerfeld 2008] increases the pressure drop, which is due to the higher energy loss by the particles in striking the wall. Also, increasing momentum exchange between the fluid and the particles leads to a higher pressure drop. Most of these simulation studies have assumed spherical particles.

The dynamics of spherical and non-spherical particles are clearly quite different and, as such, choice of appropriate fluid drag model is essential in predicting pressure drop. Probably, the most widely used expression for fluid drag on a non-spherical particle is that proposed by Haider and Levenspiel [Haider and Levenspiel 1989]. The drag coefficient for a non-spherical particle is defined as a function of the particle Reynolds number and its sphericity. Other authors have proposed using projected area of particle in the direction of flow and perpendicular to it, for evaluation of the drag coefficient [Ganser 1993, Holzer and Sommerfeld 2008]. In general, fluid drag tends to increase with decreasing particle sphericity.

Even though many researchers have pointed out that the pressure drop in pneumatic conveying is dependent on particle properties, but this topic has received very little attention. Very often information regarding particle properties such as coefficients of friction and restitution are not given along with the experimental data. We will show in this paper how particle properties affect pressure drop predictions in a DEM-CFD simulation. The commercial CFD software STAR-CD (DEM module v.1.00.111) has been used in the current study.

MODEL DESCRIPTION

The two-phase problem used to study pneumatic conveying was setup using STAR-CD. Figure 1 shows the geometry of the pipe used in the study. The two-phase gas-solid flow problem was solved employing the DEM-CFD methodology. Fluid flow is modelled using the standard Navier-Stokes equations and k-epsilon model and the solid particles using DEM. Fluid time step was taken as 1E-3 and the DEM time step as 1E-5 for the calculations presented in this paper.

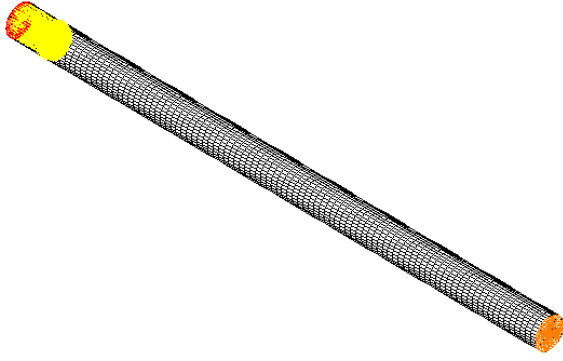


Figure 1: Geometry of pipe used in the study.

The STAR-CD DEMCFD model is based on the soft sphere modelling approach. Linear momentum balance on a particle may be written as:

$$m_i \frac{d\vec{v}_i}{dt} = m_i \vec{g} + \vec{F}_{Wall-Particle} + \vec{F}_{Particle-Particle} + \vec{F}_{FluidDrag} \quad [1]$$

where, $\vec{F}_{Wall-Particle}$, $\vec{F}_{Particle-Particle}$ are the wall-particle and inter-particle interaction forces and are modelled in STAR-CD using the soft sphere modelling technique, first used for granular flow problems by Cundall and Strack [Cundall and Strack 1979]. A linear spring dashpot model is chosen for defining inter-particle and wall-particle interactions. More about the model can be found in [STAR-CD supp. Notes, 2009].

A particle moves in the fluid domain under the influence of its body weight and fluid drag and also changes trajectory based on the collision it undergoes with other particles and system walls.

The angular momentum balance on the particle may be written as:

$$\frac{d\vec{M}_i^B}{dt} + \vec{\omega}_i^B \times \vec{M}_i^B = \vec{\tau}_i^B, \quad \vec{M}_i^B = I_i \vec{\omega}_i^B \quad [2]$$

$$\vec{\omega}_i^S = R^{-1} \vec{\omega}_i^B$$

where R is the rotation matrix for the particle, and suffix 'B' and 'S' refer to body and space fitted coordinates for the particle.

For a spherical particle, the above expression simply reduces to

$$I_i \frac{d\vec{\omega}_i}{dt} = \vec{\tau}_i \quad [3]$$

In STAR-CD DEM, a non-spherical particle is defined by method of bonded spheres [Dzyuigs and Peters, 2001]. Different spheres of same or different dimensions are combined or joined together in a desired sequence so as to form a non-spherical shape. At all times, the position of all the individual spheres in a shape remains fixed with respect to each other. To define a shape in DEM in STAR-CD, the user needs to specify the centre of mass and diameter of the individual spheres making up the non-

spherical shape. Generally, more the number of spheres used, better is the approximation to a real world shape. But, as the number of particles used in defining a shape increases, the CPU time for the simulation also increases.

The fluid present in the surroundings also influences the motion of a particle. The fluid drag on a particle can be defined using the expression:

$$F_{FluidDrag} = \frac{1}{2} C_D \rho_f A_p |v_f - v_i| (v_f - v_i) \quad [4]$$

where the drag coefficient may be defined using the general expression:

$$C_D = \frac{24}{Re} (1 + A \times Re^B) + \frac{C}{1 + \frac{D}{Re}} \quad [5]$$

For a non-spherical particle, coefficients A, B, C and D are a function of particle sphericity [Haider and Levenspiel 1989].

In STAR-CD DEM module, the default (or "standard") fluid drag model for spherical particle has the coefficients set to:

$$A = 0.15$$

$$B = 0.687$$

$$C = 0.0$$

$$D = 0.0$$

When a non-spherical particle is used for simulation, the drag coefficient is calculated based on the sphericity of the particle.

Fluid drag on a spherical particle is also defined in literature by some researchers using the correlation of Di Felice, which gives fluid drag as:

$$C_D = \frac{24}{Re} \left(0.63 + \frac{4.8\sqrt{\epsilon_f}}{\sqrt{Re}} \right)^2 \quad [6]$$

And

$$F_{FluidDrag} = \frac{1}{2} C_D \rho_f A_p |v_f - v_s| (v_f - v_s) \mathcal{E}_f^\psi \quad [7]$$

where

$$\psi = - \left[3.7 - 0.65e^{-\frac{1}{2} \left(1.5 - \log \frac{Re}{\epsilon_f} \right)^2} \right]$$

The \mathcal{E}_f^ψ factor is to account for the presence of other particles around the particle under consideration. According to the Di Felice model, the description of the drag force on a particle needs to take into account the presence of other neighbouring particles. The drag on a particle is increased due to the presence of other particles around it. This effect is modelled by introducing the porosity term in drag force expression. The porosity (local) is calculated based on the neighbours of a particle. For a non-spherical particle, such effects are not modelled

in STAR-CD DEM. For a spherical particle, it is relatively simple to evaluate porosity around a particle based on simple geometry calculations.

When fluid and particles come in contact, they exchange momentum. The particle experiences a drag force, as described above, and the fluid provides energy to the particles to be conveyed. From Newton's 3rd law, force acting on particle(s) due to fluid drag is equal and opposite to force acting on fluid due to the particles. As such, force acting on a fluid volume due to all particles is given by sum of all $F_{FluidDrag}$ vectors (opposite in sign) of particles lying in that particular fluid volume. All particle data in STAR-CD DEM is evaluated in an imaginary Lagrangian mesh (like porosity and source terms to fluid) which are then mapped on to the fluid mesh. As shown in figure 2, particle i1-i6 lies (partially or fully) in the lagrangian mesh element, as shown by the dotted lines. Drag forces acting on particle i1-i6 (multiplied by fraction of particle lying inside the mesh) are added to the lagrangian mesh element and the source term to fluid phase evaluated. Similarly, it is easy to evaluate porosity in the mesh element, which is then later mapped to the fluid mesh element.

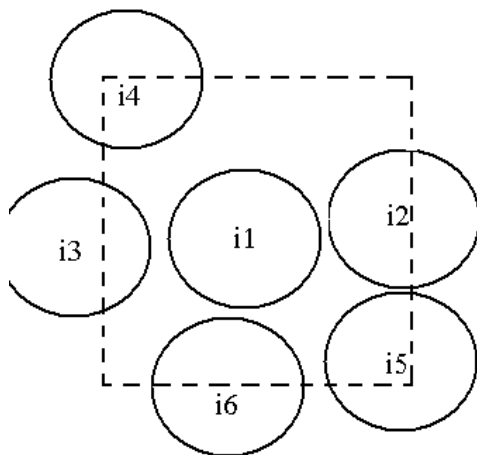


Figure 2: Evaluation of fluid-particle source terms and porosity in lagrangian mesh element.

Fluid time step can be chosen to be different from DEM time step. For a given fluid time step, one or a number of DEM time steps may be carried out (depending on their relative values) assuming fluid values or properties to be fixed during a particular DEM time step.

RESULTS

Simulations were carried out to study pressure drop in diluted pneumatic conveying in a horizontal pipe having an internal diameter of 52 mm. Simulation results were compared against the experimental data for spherical [Marcus *et al*, 1990] and ellipsoidal [Vasquez *et al*, 2008] particles, at different particle and gas flow rates. Particle outlet velocities were also compared with the experiments.

It should be noted that, in the literature for pneumatic conveying, the experimental values of the particle physical properties and shape are not always available. For the simulation results that we have used in this study, the values for coefficients of restitution and friction between

particle-particle and the particle-wall were not available. The values we have assumed are listed in Table 1, unless otherwise mentioned.

Property	Spherical particle	Ellipsoidal particle
Diameter (mm)	2.385	4
Density (kg/m ³)	1050	
Coeff. of restitution (particle-particle and particle-wall)	0.8	0.8
Coeff. of friction (wall-particle and particle-particle)	0.3	0.3
Fluid drag model	Standard	Haider and Levenspiel

Table 1: Default DEM modelling parameters

In this study of two-phase flow through pipe, it has been assumed in all the simulations that the particles injected into the pipe are uniformly distributed across the pipe inlet. Generally, in most experimental conveying systems, mass of solid is fed from a hopper or storage bunker into a chamber from where the fluid entrains the particles into the pipe [Tsuji and Morikawa, 1982]. We do not include such features in the current study and assume the particles to be uniformly distributed at the pipe inlet. For a non-spherical particle case, the orientation of the particle at the inlet is also chosen randomly.

Figure 3 shows the pressure drop in pipe with mono-sized spherical particles being injected at a rate of 251 kg/hr. It can be seen that the pressure drop increases with increasing fluid velocity, as expected. The match between experiments and simulation is found to be reasonable. As has been mentioned earlier, in absence of information about particle properties, a restitution coefficient of 0.9 was assumed for the spherical particles in this case.

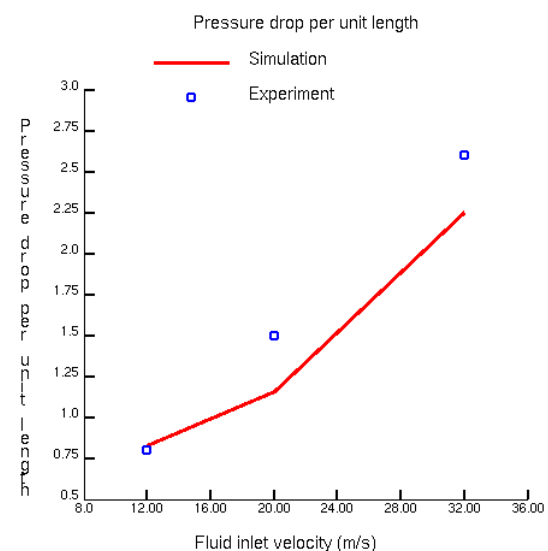


Figure 3: Pressure drop per unit length of pipe for 251-kg/hr solid loading cases.

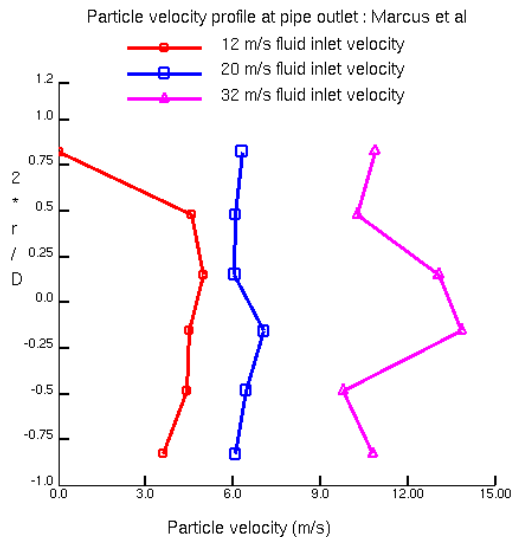


Figure 4: Solid axial velocity profile at pipe outlet, for 251-kg/hr solid loading cases.

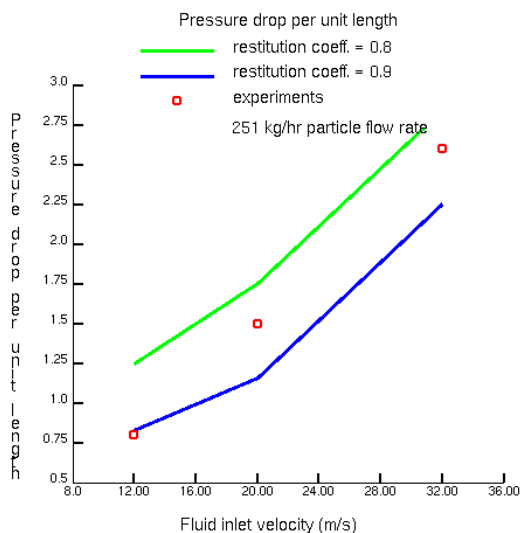


Figure 5: Pressure drop per unit length of pipe for 251-kg/hr solid loading cases, with different restitution coefficient.

Figure 4 shows particle velocity profile at the pipe outlet for the three different cases. The particle velocity profiles are more or less flat and show no specific trend. The particle velocity near the walls is a little lower than that at the pipe centre. This is because the particles near the wall may undergo a higher number of collisions, than those in the core. The more the number of collisions of a particle, the more is the energy required by fluid to convey the particles leading to higher-pressure drops.

Figure 5 shows the pressure drop in the pipe when the particle restitution coefficient is assumed to be a little lower at around 0.8 (both wall-particle and particle-particle coefficient of restitution). It can be seen that the pressure drop is higher for the 0.8 restitution coefficient cases than for 0.9 restitution coefficient cases. This could be due to the fact that in 0.8 restitution coefficient cases, the particle loses more energy per collision. Also, as the particle loses more energy per collision, it may also undergo more collisions compared to 0.9 restitution coefficient cases. That is to say, a particle with restitution

coefficient 0.9 may exit a pipe after, say n collisions, but the particle with restitution coefficient 0.8 may exit the pipe after, say $n+20$ collisions. We hence analyse collision data of particles for 32 m/s fluid inlet velocity case, with 0.8 and 0.9 as restitution coefficients. It is found that the total number of wall-particle and particle-particle collisions for all particles in the two cases differs. The total number of collision that had taken place in the pipe after a given period of time was higher when restitution coefficient was chosen as 0.8, rather than 0.9. Thus, with a lower restitution coefficient, there are an increased number of collisions taking place, coupled with an increased energy loss per collision, leading to higher pressure drop in the system.

Another important factor that may influence prediction of pressure drop is the choice of the fluid drag model. For spherical particles, a number of fluid drag models exist in the STAR-CD DEM module. By default, the standard drag model in STAR-CD DEM is selected during simulations. Another model widely used is that of Di Felice [STAR-CD supp. Notes, 2009]. It is similar to the standard drag model, except for the additional term to account for the porosity around the particle, and the particle Reynolds number. Most of the drag coefficients defined are based on settling of a single particle. Di Felice modified the form of fluid drag expression to take into account the higher drag when particles are large in number and drag on a particle is affected by presence of other particles around.

Figure 6 shows model prediction for pressure drop with the two different fluid drag models – the standard fluid drag model and the Di Felice model. As expected, there is very little difference between the predictions from these two models. The case studied deals with lean mixture only; the particle concentration correction factor in the Di Felice model is small and made no noticeable difference in the pressure drop prediction. Probably, the choice of Di Felice model would become important when dealing with dense or slug flows. It may be concluded that for diluted flows, choice of fluid drag model is not that important.

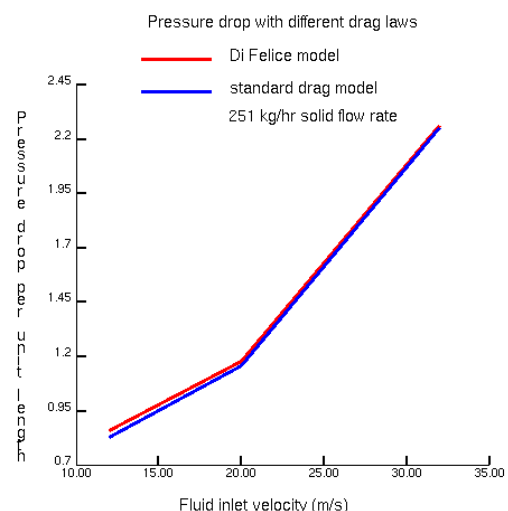


Figure 6: Pressure drop per unit length of pipe for 251-kg/hr solid loading cases, with different fluid drag laws.

Particle shape also plays an important role in defining the pressure drop. Drag on a particle increases with decreasing particle sphericity and as such, the momentum exchange

with the fluid increases resulting in a higher pressure drop. For a non-spherical particle, we employ the drag coefficient proposed by Haider and Levenspiel. Simulations were carried out based on the experimental setup as defined in Vasquez et al [Vasquez et al 2008]. Vasquez et al have presented pressure drop in vertical as well as horizontal pipes with soft and hard pellets. Here, we confine our attention to horizontal pipes with soft pellets only. Ellipsoidal particles were used during the experiments with an effective diameter of 4 mm. The shape of the ellipsoid was defined using method of bonded spheres in STAR-CD. Typical shape of the particles used in the simulation is shown in Figure 7.

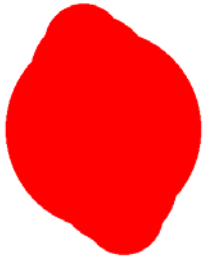


Figure 7: Typical shape of an ellipsoidal particle assumed in the current study. Combining multiple spheres of different diameter forms particle.

As mentioned in the section for Model Description, a non-spherical particle is formed by combining together a number of spherical particles. These individual spherical particles can overlap extensively with each other and their positions with respect to each other are defined so as to model the appropriate shape. In the results of Vasquez et al, the exact shape of the ellipsoid is not mentioned and so we assume a shape as shown in the figure 7, with an effective diameter of 4 mm.

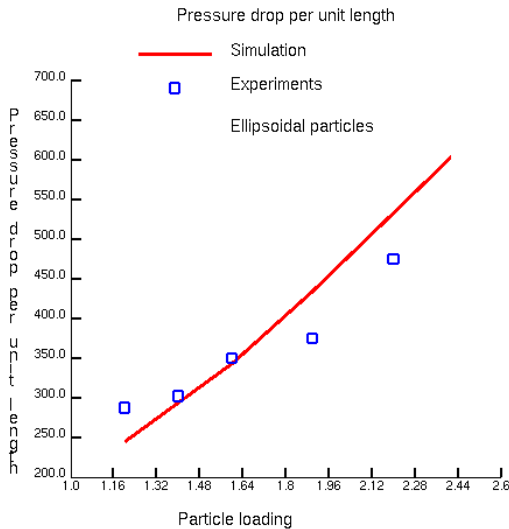


Figure 8: Pressure drop per unit length of pipe for soft ellipsoidal particles at different solid loadings.

Simulation studies were carried out using soft ellipsoidal particles at 15.3 m/s gas flow rate and different particle loadings. The particle restitution coefficient was assumed to be 0.8 (no values provided from the experiment). Figure 8 shows pressure drop in the pipe at varying particle loadings. It can be observed that STAR-CD DEM is able to reproduce pressure drop in the pipe with reasonable

accuracy. As the particle loading increases, the pressure drop along the pipe increases. Increasing particle loading increases the number of particle collisions in the pipe and in turn increasing the pressure drop. Figure 9 shows a plot of the percentage of total number of wall-particle collisions (= total number of wall particle collisions / {total number of wall-particle collisions+ total number of particle-particle collisions}) that have taken place in the pipe till 1.8 seconds, at different particle loadings. It can be seen that the percentage of wall particle collision decreases with increasing particle loading. Though the total number of collisions increases with increasing particle loading, the increase of number of particle-particle collisions is greater than the increase of wall-particle collisions. Still, a value of over 65% for percentage of wall particle collisions points to a dilute flow. In a dense flow, one may expect this percentage of wall particle collisions to be much lower.

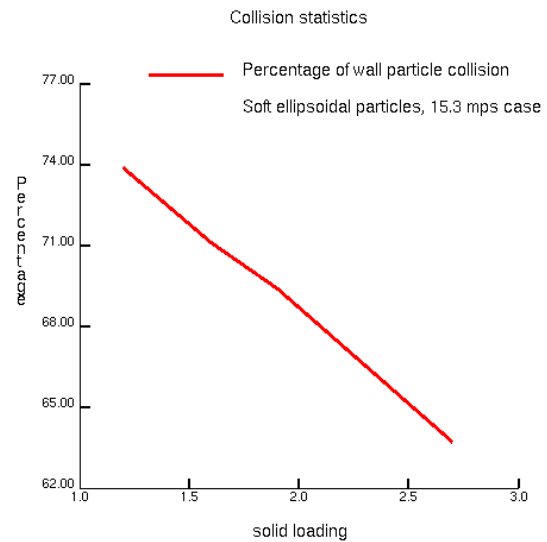


Figure 9: Percentage of wall-particle collisions after time 1.8 seconds with ellipsoidal particles and different solid loadings.

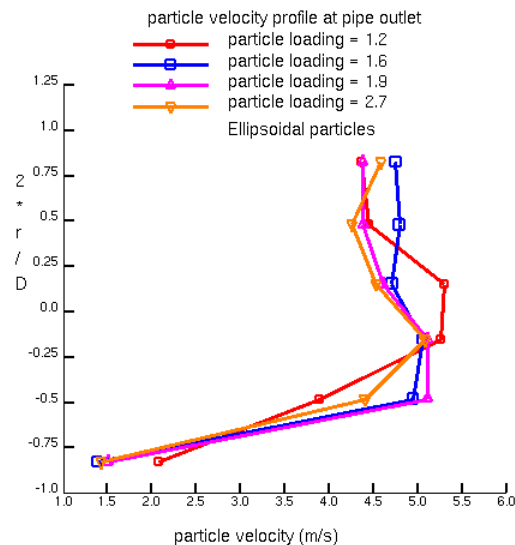


Figure 10: Particle velocity profile at pipe outlet, for soft ellipsoidal particles at different solid loadings.

The good match of experimental data for pressure drop with simulations lends credibility to the DEM predictions for dilute conveying.

Also, one may compare particle axial velocities at the pipe outlet. Vasquez et al have reported an almost constant value of 5 m/s for particle velocity magnitude at pipe outlet, for all particle loadings. The plot of particle velocity profile at the pipe outlet, for different particle loadings, is shown in figure 10. It can be seen that the predictions from DEM are again very good. The predicted particle velocities are near the 5 m/s mark, at all particle loadings. As expected, the particle velocity at the bottom of the pipe is low and is due to higher number of wall-particle collisions there.

CONCLUSION

STAR-CD DEM module is able to predict pressure drop in dilute pneumatic conveying with reasonable accuracy. The pressure drop increases with increasing solid loading as well as increasing fluid velocity. Particle velocity profile at the pipe outlet is also in good agreement with the experiments. It is found that the percentage of wall particle collisions decrease with respect to particle-particle collisions, as the solid loading is increased. The number of particle collisions is also sensitive to particle properties. Hence, it is very important to set proper parameters for the particle before running a DEM simulation. Much of the data available in the literature does not contain information about particle properties and shape and hence care must be taken while reporting such data.

REFERENCES

- CUNDALL P. A. and STRACK O. D. L., (1979), "A discrete numerical model for granular assemblies", *Geotechnique*, 29, 47 – 65.
- DZIUGYS A and PETERS B, (2001), "An approach to simulate the motion of spherical and non-spherical fuel particles in combustion chambers", *Granular Matter*, 3, 231- 265.
- GANSER G. H., (1993), "A rational approach to drag prediction of spherical and non-spherical particles", *Powder Technology*, 77, 143 – 152.
- HAIDER A. and LEVENSPIEL O., (1989), "Drag coefficient and terminal velocity of spherical and non-spherical particles", *Powder Technology*, 58, 63 – 70.
- HOLZER A. and SOMMERFELD M., (2008), "New simple correlation formula for the drag coefficient of non-spherical particles", *Powder Technology*, 184, 361 – 365.
- LAIN S. and SOMMERFELD M., (2008), "Euler / Lagrange computations of pneumatic conveying in a horizontal channel with different wall roughness", *Powder Technology*, 184, 76 – 88.
- MARCUS et al, (1990), "Pneumatic conveying of solids", Chapman and Hall.
- STAR-CD supplementary notes, Chapter 23, Discrete Element Modelling, CD-adapco.
- TSUJI Y and MORIKAWA Y, (1982), "LDV measurements of an air-solid two-phase flow in a horizontal pipe", *Journal of Fluid Mechanics*, 120, 385 – 409.
- VASQUEZ et al, (2008), "Visual analysis of particle bouncing and its effect on pressure drop in dilute phase pneumatic conveying", *Powder Technology*, 179, 170 – 175.